2′-Deoxyriboguanylurea, the primary breakdown product of 5-aza-2′-deoxyribocytidine, is a mutagen, an epimutagen, an inhibitor of DNA methyltransferases and an inducer of 5-azacytidine-type fragile sites

Katarzyna Lamparska[1], Jarrod Clark[1], Gail Babilonia[1], Victoria Bedell[2], Wesley Yip[1] and Steven S. Smith[1],*

[1]Beckman Research Institute and Division of Urology and Urologic Oncology and [2]Cytogenetic Core of the City of Hope Comprehensive Cancer Center, City of Hope, 1500 E. Duarte Rd., Duarte, CA 91010-3000, USA

ABSTRACT

5-Aza-2′-deoxycytidine (5azaC-dR) has been employed as an inhibitor of DNA methylation, a chemotherapeutic agent, a clastogen, a mutagen, an inducer of fragile sites and a carcinogen. However, its effects are difficult to quantify because it rapidly breaks down in aqueous solution to the stable compound 2′-deoxyriboguanylurea (GuaUre-dR). Here, we used a phosphoramidite that permits the introduction of GuaUre-dR at defined positions in synthetic oligodeoxynucleotides to demonstrate that it is a potent inhibitor of human DNA methyltransferase 1 (hDNMT1) and the bacterial DNA methyltransferase (M.*Eco*RII) and that it is a mutagen that can form productive base pairs with either Guanine or Cytosine. Pure GuaUre-dR was found to be an effective demethylating agent and was able to induce 5azaC-dR type fragile sites FRA1J and FRA9E in human cells. Moreover, we report that demethylation associated with C:G → G:C transversion and C:G → T:A transition mutations was observed in human cells exposed to pure GuaUre-dR. The data suggest that most of the effects attributed to 5azaC-dR are exhibited by its stable primary breakdown product.

INTRODUCTION

5-Azacytidine (5azaC-R) is a multifaceted drug that has been characterized as a mutagen (1–3), clastogen (4), carcinogen (5) and epimutagen in mammalian cells (6). It can elicit massive chromatin restructuring (7,8), and can elicit re-expression of silent genes regardless of their promoter methylation state (9). These effects are thought to be associated with its capacity to produce demethylated DNA via *in vivo* reduction to 5-aza-2′-deoxycytidine (5azaC-dR) and incorporation into DNA, where its capacity for epigenetic and genetic damage (10) is associated with the trapping (11) and subsequent destruction of DNA methyltransferase 1 (12).

The lability of both 5azaC-R and 5azaC-dR in aqueous media is well known. Both are rapidly hydrolyzed to the 2′-deoxyriboguanylurea forms (GuaUre-R and GuaUre-dR) in aqueous media at neutral pH (13) with a half-life of about 10 h. Its half-life in DNA is predicted to be slightly longer although reliable measurements of its stability in DNA are unavailable. Direct evidence for the presence of 5azaC in DNA isolated from prokaryotic or eukaryotic cells exposed to either 5azaC-R or 5azaC-dR has not been obtained. Incorporation into DNA has been inferred from the more pronounced biological effects of 5azaC-dR compared with 5azaC-R (14) and the capacity of isolated DNA to contain tightly bound proteins (15). The genetic evidence is consistent with the predicted chemical breakdown since both 5azaC-R and 5azaC-dR mutagenesis produces a significant number of C:G → G:C transversion and C:G → T:A transition mutations in both bacteria (1) and mammals (10). Transversions are best explained by the capacity of GuaUre-dR in DNA to pair with cytosine as proposed by Jackson-Grusby *et al.* (10), while the transition mutations are consistent with either bypass synthesis after glycolytic removal of GuaUre-dR or mispairing of GuaUre-dR or 5azaC-dR with dA.

In principle, GuaUre-dR could be generated by the breakdown of 5azaC-R incorporated as a cytidine analog forming a GuaUre-dR:dG mispair. Alternatively,

---

it could be incorporated directly into DNA as an analog of either deoxycytidine or deoxyguanine. Most protocols (16) employing 5azaC-R to study bacterial cells require exposure to the drug over a short period (1–5 h). Thus, 5azaC-R incorporated into DNA as a cytidine analog is expected to account for the bulk of the incorporation in these experiments. In contrast, 5azaC-R protocols for studies in eukaryotic cells require prolonged exposure (24–72 h) to 1 μM drug in aqueous solution where it is rapidly hydrolyzed to GuaUre-dR that may be incorporated directly into DNA.

Here, we report synthetic approaches to the production of pure GuaUre-dR, its phosphoramidite, and oligodeoxynucleotides containing GuaUre-dR at preselected sites. We used these syntheses to show that GuaUre-dR in DNA was a potent inhibitor of Human DNA Methyltransferase 1 (hDNMT1) and the bacterial DNA methyltransferase (M.*Eco*RII), and that direct exposure of human cells to GuaUre-dR can produce both demethylation (epimutation) and mutation. Direct exposure of human cells to GuaUre-dR was also found to mimic the ability of 5azaC-dR in the induction of fragile sites FRA1J and FRA9E that were previously thought to be uniquely induced by 5azaC-R or 5azaC-dR. We used PCR mapping to study the base-pairing spectrum generated during amplification at sites of GuaUre-dR incorporation in the template strand. Those results suggest that GuaUre-dR mediated mutagenesis mimics 5azaC-R and 5azaC-dR mediated mutagenesis in that it produces both C:G → G:C transversions and C:G → T:A transitions.

MATERIALS AND METHODS

Reagents

Phosphoramidite synthesis (overview)

We noted that GuaUre oligodeoxynucleotides are not stable during standard ammonium deprotection. Thus, *p*-nitrophenylethyl (NPE) and *p*-nitrophenylethoxycarbonyl (NPEOC) protecting groups (17) were used in the synthesis of the GuaUre-dR phosphoramidite. The NPEOC protected phosphoramidite of GuaUre-dR (Figure 1) was prepared by transglycosylation of 5′,3′-O-(1,1,3,3-tetraisopropyldisiloxane-1,3-diyl)-2′-deoxyuridine (13) with silylated 5-azacytosine in the presence of trimethylsilyl trifluoromethansulfonate as the catalyst in anhydrous DCM. The β-anomer of 5′,3′-O-(1,1,3,3-tetraisopropyldisiloxane-1,3-diyl)-5-aza -2′-deoxycytidine, was separated from the remaining substrate and from the α-amoner by silica gel chromatography. Ammonium hydroxide treatment of triazine ring gave the required GuaUre intermediate. Acylation at the amino positions of GuaUre was achieved by reaction with excess of 2-(4-nitrophenyl)-ethyl chloroformate (17). The removal of 5′,3′-TIPDS-protecting groups, was performed with tetra-n-butylammonium fluoride or TAS-F (18). Use of more stable TIPDS instead of commonly employed trimethylsilyl group helped with α,β-anomer separation during silicagel purification (19). Reactions of NPEOC protected GuaUre-dR with DMTr-Cl followed by

reaction with bis-[*N,N*-diisopropylamino-2-(4-nitrophenyl)]ethoxyphosphane (19) gave the required phosphoramide. The remaining NPE, NPEOC-phosphoramidites were prepared as described in (17,20). Direct synthesis of 5′-*O*-dimethoxytrityl -3′-*O*-[2-(4-nitrophenyl)ethoxy-*N,N*-diisopropyl] -2′-deoxyribofuranosyl-3-guanyl-*N,N*-bis-[2-(4-nitrophenyl)ethoxycarbonyl]-urea phosphoramidite is described below.

Phosphoramidite synthesis (experimental)

5′,3′-O-(1,1,3,3-tetraisopropyldisiloxane-1,3-diyl)-2′-deoxyuridine (1). A mixture of 2′-deoxyuridine (2.28 g, 10 mmol) and 1,3-dichloro-1,1,3,3-tetraisopropyldisiloxane (3.47 g, 3.52 ml, 11 mmol) in 60 ml of dry pyridine was stirred at room temperature for 24 h. The reaction mixture was dried under the vacuum and co-evaporated twice with toluene to remove the reminder of pyridine. The residue was dissolved in dichloromethane (DCM) (100 ml) and washed with water, dried under Na_2SO_4. The filtrates were combined and evaporated to dryness in vacuum. The residue was purified on a silica gel column (DCM/MeOH with 2% MeOH) to give 3.38 g of pure product **1** as foam with 91% yield.

R_f = 0.49 (DCM/MeOH 95/5); MS expected: 470.23, *m/z* found: 470.91 (MH$^+$), 940.73 (2MH$^+$).

β-5′,3′-O-(1,1,3,3-tetraisopropyldisiloxane-1,3-diyl)-2′-deoxy-5-azacytidine (2a). Product **1** (1.88 g, 4 mmol) and 5-azacytosine (1.12 g, 10 mmol) were suspended in anhydrous DCM (100 ml) followed by *N,O*-bis(trimethylsilyl)trifluoroacetamide (13.4 ml, 50 mmol) and refluxed for 3 h under an argon atmosphere, until the suspension was mostly dissolved. After the reaction mixture was cooled to room temperature trimethylsilyl trifluoromethanesulfonate (2.72 ml, 15 mmol) was added and the reaction was refluxed for additional 6 h under an argon atmosphere. It was then diluted with 60 ml of DCM and extracted with an ice-cold solution of brine. The organic layer was dried (Na_2SO_4) and the solvents were removed under reduced pressure. The β-anomer was separated from remaining substrate and α-anomer using a silica gel column DCM/MeOH with 1–2% MeOH, giving pure β-TIPDSi-5azaC-dR with 25% yield.

R_f = (β-TIPDSi-5azaC-dR) = 0.52 (ethyl acetate/ethanol 49/1); MS expected: 470.24, *m/z* found: 493.38 (MNa$^+$), 941.46 (2MH$^+$), 963.31 (2MNa$^+$), 1432.91 (3MNa$^+$), 1903.46 (4MNa$^+$); ^{1}H NMR (CDCl$_3$) δ (ppm): 8.45 (s, 1H, H-6), 6.00 (t, 1H, H-1′), 5.8 (s, 1H, NH$_A$), 5.44 (s, 1H, NH$_B$), 4.41 (m, 1H, H-3′), 4.14 (m, 1H, H-4′), 3.99 (m, 1H, H-5′), 3.78 (m, 1H, H-5″), 2.53 (m, 1H, H-2′), 2.36 (m, 1H, H-2″), 0.9–1.10 (m, 28 H, CHMe$_2$); R_f = (α-TIPDSi-5azaC-dR) = 0.45 (ethyl acetate/ethanol 49/1), MS expected: 470.24, *m/z* found: 941.48 (2MH$^+$), 1433.7 (3MNa$^+$).

5′,3′-O-(1,1,3,3-tetraisopropyldisiloxane-1,3-diyl)-2′-deoxyribofuranosyl-3-guanylurea (3). Product **2a** (750 mg, 1.59 mmol) was dissolved in 20 ml of mixture dioxane/methanol (1/1) followed by 10 ml of 25% NH$_4$OH and stirred overnight at room temperature. After TLC analysis (DCM/MeOH 9/1) the mixture was evaporated
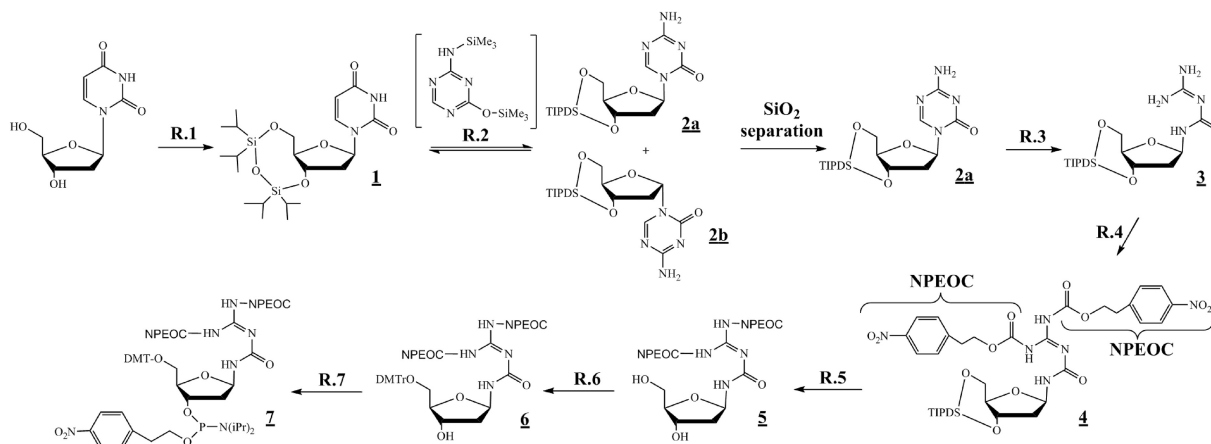
Figure 1. Synthesis of the phosphoramidite for GuaUre-dR **7**. R.1: 2′-Deoxyuridine, 1,3-dichloro-1,1,3,3-tetraisopropyldisiloxane in Py anh., product: 5′,3′-*O*-(1,1,3,3-tetraisopropyldisiloxane-1,3-diyl)- 2′-deoxyuridine **1** ($Y = 91\%$); R.2: **1**, 5-azacytosine, *N,O*-bis(trimethylsilyl)trifluoro-acetamide, trimethylsilyl trifluoromethanesulfonate in DCM, products: mixture of, α,β anomers of 5′,3′-*O*-(1,1,3,3-tetraisopropyldisiloxane-1,3-diyl)- 2′-deoxy-5-azacytidine β-**2a** ($Y = 25\%$), α-**2b** ($Y = 25\%$); SiO$_2$ separation of β-**2a** and α-**2b** anomers; R.3: β-**2a**, 25% NH$_4$OH/dioxane/methanol (1/2/2), product: 5′,3′-*O*-(1,1,3,3-tetraisopropyldisiloxane-1,3-diyl)- 2′-deoxyribofuranosyl-3-guanylurea **3**; R.4: **3**, 2-(4-nitrophenyl)ethyl chloroformate in Py anh., product: 5′,3′-*O*-(1,1,3,3-tetraisopropyldisiloxane-1,3-diyl)- 2′-deoxyribofuranosyl -3-guanyl-*N,N*-bis-[2-(4-nitrophenyl)-ethoxycarbonyl]-urea **4** ($Y = 64.6\%$); R.5: **4**, 1 M tetrabutylammonium fluoride (TBAF) in THF, product: 2′-deoxyribofuranosyl-3-guanyl-*N,N*-bis-[2-(4-nitrophenyl)ethoxycarbonyl]-urea **5** ($Y = 65\%$); R.6: **5**, dimethoxytrityl chloride in pyridine, product: 5′-*O*-dimethoxytrityl-2′-deoxyribofuranosyl-3-guanyl-*N,N* bis-[2-(4-nitrophenyl)ethoxycarbonyl]-urea **6** ($Y = 56\%$); R.7: **6**, bis-(*N,N*-diisopropylamino)-2-(4-nitrophenyl) ethoxyphosphane, 1H-tetrazole in DCM, Et$_3$N after reaction, product: 5′-*O*-dimethoxytrityl-3′-*O*-[2-(4-nitrophenyl)ethoxy-*N,N*-diisopropyl]-2′-deoxyribofuranosyl-3-guanyl-*N,N*-bis-[2-(4-nitrophenyl)ethoxycarbonyl]-urea phosphoramidite **7** ($Y = 50\%$).

to dryness under vacuum and processed further without purification.

MS expected: 460.25; m/z found: 461.26 (MH$^+$), 921.52 (2MH$^+$)

5′,3′-O-(1,1,3,3-tetraisopropyldisiloxane-1,3-diyl)-2′-deoxyribofuranosyl-3-guanyl-N,N-bis-[2-(4-nitrophenyl) ethoxycarbonyl]-urea (4). Product **3** (733 mg, 1.59 mmol) was dried by twice co-evaporation with anhydrous pyridine, reacted with 2-(4-nitrophenyl)ethyl chloro-formate (2190.4 mg, 9.54 mmol) in anhydrous pyridine (20 ml) and stirred overnight at room temperature. After TLC analysis, the reaction was evaporated to dryness and twice co-evaporated with toluene to remove traces of pyridine. The residue was dissolved in DCM, washed with 1 M sodium bicarbonate, dried (Na$_2$SO$_4$) and concentrated to dryness. The residue was purified on a silica gel column in DCM/MeOH (0.5% MeOH) to give pure product **4** with 64.6% yield.

$R_f = 0.66$ (DCM/MeOH 95/5); MS expected: 846.33; m/z found: 847.18 (MH$^+$), 869.18 (MNa$^+$), 1714.82 (2MNa$^+$).

2′-Deoxyribofuranosyl-3-guanyl-N,N-bis-[2-(4-nitrophenyl) ethoxycarbonyl]-urea (5). To product **4** (800 mg, 0.94 mmol) dissolved in anhydrous tetrahydrofuran (THF) (30 ml), 1.42 ml of 1 M tetra-*n*-butylammonium fluoride in THF (1.42 mmol) was added drop-wise and stirred for a few minutes. After total deprotection (5 min), the reaction was concentrated to dryness and purified on a silica gel column in DCM/MeOH (3% MeOH) giving product **5** with 65% yield.

$R_f = 0.46$ (DCM/MeOH 95/5); MS expected: 604.18; m/z found: 627.09 (MNa$^+$), 1230.73 (2MNa$^+$).

5′-O-dimethoxytrityl-2′-deoxyribofuranosyl-3-guanyl-N, N-bis-[2-(4-nitrophenyl)ethoxycarbonyl]-urea (6). Product **5** (380 mg, 0.63 mmol) was dried by twice co-evaporation with anhydrous pyridine and reacted with dimethoxytrityl chloride (426.2 mg, 1.26 mmol) in anhydrous pyridine (10 ml). The reaction was stirred over-night at room temperature while covered with aluminum foil to protect it from light. After that, the reaction was evaporated to dryness and twice co-evaporated with toluene to remove traces of pyridine. The residue was dissolved in DCM, washed with 1 M sodium bicarbonate, dried (Na$_2$SO$_4$) and concentrated to dryness. The residue was purified on a silica gel column in DCM/MeOH (1–3% MeOH) to give product **6** with 56% yield.

$R_f = 0.66$ (DCM/MeOH 95/5); MS expected 906.31; m/z found: 929.3 (MNa$^+$); ^{1}H NMR (CDCl$_3$) δ (ppm): 8.18 (m, 4H, Ar, NPEOC), 7.38 (m, 4H, Ar, NPEOC), 7.0–7.3 (m, 9 H, Ar, DMT), 6.81 (m, 4H, Ar, DMT), 4.43 (m, 5 H, H-3′, CH$_2$ NPEOC), 3.89 (m, 1H, H-4′), 3.80 (s, 6H, Me, DMT), 3.60 (m, 2H, H-5′), 3.11 (m, 4H, CH$_2$ NPEOC), 2.1 (m, 2H, H-2′, 2″).

5′-O-dimethoxytrityl-3′-O-[2-(4-nitrophenyl)ethoxy-N, N-diisopropyl]-2′-deoxyribofuranosyl-3-guanyl-N,N-bis-[2-(4-nitrophenyl)ethoxycarbonyl]-urea phosphoramidite (7). Product **6** (330 mg, 0.355 mmol) was dried by co-evaporation with anhydrous DCM. The residue was dissolved in 3.3 ml of anhydrous DCM followed by addition of bis-(*N,N*-diisopropylamino)-2-(4-nitrophenyl)-ethoxyphosphane (282.2 mg, 0.71 mmol) in DCM (2 ml) and 394 μl (0.18 mmol) of 0.45 M 1-H-tetrazole in anhyd-rous CH$_3$CN. After stirring overnight, the TLC analysis showed the formation of the desired product, 0.1 ml of triethylamine was added and the mixture was diluted

with 100 ml of 5% Et_3N in DCM and washed with saturated $NaHCO_3$. The organic layer was dried over Na_2SO_4 and evaporated to dryness. The residue was purified by silica gel column chromatography in hexane/EtOAc/Et_3N (50/49/1) and lyophilized in benzene to give product **7** with 50% yield.

$R_f = 0.68$ (hexane/EtOAc 1/1); MS expected: 1202.44; m/z found: 1225.18 $(MNa)^+$; ^{31}P-NMR $(CDCl_3) = 147.69$, 147.31.

Supporting reagents

Bis-(N,N,-diisopropylamino)-2-(4-nitrophenyl)ethoxy-phosphane;
^{31}P-NMR $(CDCl_3) = 122.53$.

5'-O-dimethoxytrityl -3'-O-[2-(4-nitrophenyl)ethoxy-N,N-diisopropyl]- 2'-deoxy-N^4-[2-(4-nitrophenyl)ethoxy-carbonyl]-cytidine-phosphoramidite
$R_f = 0.58$ (DCM/EtOAc 1/1); MS expected 1018.39; m/z found: 1019.27 (MH^+), 1041.45 (MNa^+);
^{31}P NMR $(CDCl_3) = 148.31$, 148.06.

5'-O-dimethoxytrityl-3'-O-[2-(4-nitrophenyl)ethoxy-N,N-diisopropyl]- 2'-deoxy-N^6-[2-(4-nitrophenyl)ethoxy-carbonyl]-adenosine-phosphoramidite
$R_f = 0.77$ (DCM/EtOAc 1/1); MS expected 1042.4; m/z found: 1043.2 (MH^+), 1065.28 (MNa^+);
^{31}P NMR $(CDCl_3) = 148.26$, 147.97.

5'-O-dimethoxytrityl-3'-O-[2-(4-nitrophenyl)ethoxy-N,N-diisopropyl]-2'-deoxy N^2-[2-(4-nitrophenyl)ethoxy-carbonyl]-O^6-[2-(4-nitrophenyl)ethyl]-guanosine-phosphoramidite
$R_f = 0.89$ (DCM/EtOAc 1/1); MS expected 1207.44; m/z found: 1230.43 (MNa^+);
^{31}P NMR $(CDCl_3) = 148.08$, 147.99.

5'-O-dimethoxytrityl-3'-O-[2-(4-nitrophenyl)ethoxy-N,N-diisopropyl]-2'-deoxythymidine-phosphoramidite
$R_f = 0.825$ (DCM/EtOAc 1/1); MS expected 840.35; m/z found: 841.36 (MH^+), 863.14 (MNa^+);
^{31}P NMR $(CDCl_3) = 148.13$, 147.68.

Oligodeoxynucleotide synthesis

Oligomers were prepared on the 1 μmol scale with a Cyclon Plus DNA Synthesizer using phosphoramidites with NPE and NPEOC protecting groups. Nucleosides with NPE/NPEOC (17) were attached to controlled-pore glass (CPG) through an oxalyl linkage as described in (21,22). All phosphoramidites were dissolved in anhydrous DCM to obtain a 0.04 M solution. Standard reagents and cycles were used for the synthesis with modification of coupling time from 30 s to 3 min. DMTr groups were removed after synthesis. Deprotection was carried out by using the non-nucleophilic base 1,8-diazabicyclo[5.4.0]undec-7-ene DBU (0.5 M) in anhydrous pyridine containing 5 mg thymine for 15 h at room temperature (18). The reaction was neutralized with glacial acetic acid and concentrated to dryness. The residues were washed with water and purified by HPLC. HPLC purification was performed on a PRP-1 column using

the following solutions: A: 10% acetonitrile (AcCN) in 40 mM tetrabutylammonium acetate (TBAA), pH 6.5; B: 90% AcCN in 40 mM TBAA, pH 6.5. Flow rate: 2.5 ml/min, 20 min linear gradient from 0% B to 90% B. Purity of collected 1 ml fractions was checked by PAGE. Pure fractions were combined and desalted on HPLC using the following solvents: A: 2% AcCN in 50 mM triethylammonium acetate (TEAA), pH 6.5; B: 90% AcCN in 50 mM TEAA, pH 6.5. Flow rate: 2.5 ml/min, 20 min, linear gradient from 0% B to 90% B followed by isopropanol precipitation. Oligodeoxynucleotides, containing GuaUre ran as single 30-mers on 19% denaturing PAGE. They were further characterized by mass spectrometry (MS) using electrospray $(m-z)/z$ ionization conditions.

Dodecamer I-control (5'-TTXTTTTTTTTT-3', X = GuaUre-dR): MS expected 3562.61, found 3562.7.

Dodecamer II-control (5'-CGXGAATTCGCG-3', X = GuaUre-dR); MS expected 3635.66, found 3635.7.

30-mer GuaUre-dR Targeted CCGG (5'-GTCCACCAGATCXGGGCTACCTGGCCTCGA-3', X = GuaUredR): MS expected 9115.5, found 9115.9.

30-mer GuaUre-dR Targeted CCWGG (5'-GCTGGCTATGCCACXAGGTGAGGCTAACTG-3', X = GuaUre-dR); MS expected 9234.6, found 9234.9.

All other oligodeoxynucleotides (Table 1) were synthesized using the same DNA synthesis equipment, commercially available phosphoramidites (Glen Research, Sterling, VA, USA) using standard ammonia deprotection methods. Purification was carried out as described above.

Human DNMT1 purification

HeLa S3 cells $(2.9 \times 10^9$ cells) were purchased from the National Cell Culture Center (Biovest International, Minneapolis, MN, USA). Nuclear extracts were prepared as described in (23) except that Tris buffer was used instead of HEPES to give a protein concentration of 10 mg/ml (total 85 mg of protein). The nuclear extract was then applied to ÄKTApurifier® System (GE Healthcare) using a 5 ml Hi-Trap DEAE-FF column (17 mg protein/ml, GE Healthcare) followed by a Hi-Trap SP FF (1 ml, GE Healthcare) (24). Protein was eluted with a linear gradient from 100 mM to 1 M NaCl. Fractions containing protein were pooled and applied to a hydroxyapatite column (1×1) equilibrated with buffer A: 10 mM KPi, 50 mM Tris–Cl pH 7.8, 0.08 mM EDTA, 2.5 mM βME, 25% v/v glycerol. The column was washed with 10 ml of the same buffer and eluted with buffer B: 500 mM KPi 50 mM Tris–Cl pH 7.8, 0.08 mM EDTA, 2.5 mM βME, 25% v/v glycerol). Enzyme activity was measured as previously described (25). The purified enzyme had a specific activity of 20.96 fmol/min/mg.

M.*Eco*RII purification

*Eco*RII-Trx (BL21 cells) were grown following the procedure described in (26) using Super Broth medium with AMP50. After reaching 0.8 OD600 they were induced with 1 M IPTG. A total of 100 g of *Eco*RII-Trx cells were suspended in 500 ml of Buffer A (10 mM Potassium

Table 1. Sequences of 30mer duplex oligodeoxynucleotides

Duplex	Sequences
S_0	De Novo CCWGG Duplex 5´-CAGTTAGCCTCA<u>CCTGG</u>TGGCATAGCCAGC-3´ 3´-GTCAATCGGAGT<u>GGACC</u>ACCGTATCGGTCG-5´
S_1	Hemimethylated Targeted CCWGG Duplex 　　　　　　　　　　M *5´-CAGTTAGCCTCA<u>CCTGG</u>TGGCATAGCCAGC-3´ 3´-GTCAATCGGAGT<u>GGACC</u>ACCGTATCGGTCG-5´
S_2	5FdC Targeted CCWGG Duplex 　　　　　　　　　　M *5´-CAGTTAGCCTCA<u>CCTGG</u>TGGCATAGCCAGC-3´ **3´-GTCAATCGGAGT<u>GGACC</u>ACCGTATCGGTCG-5´ 　　　　　　　　　　F
S_3	GuaUre-dR Targeted CCWGG Duplex 　　　　　　　　　　M *5´-CAGTTAGCCTCA<u>CCTGG</u>TGGCATAGCCAGC-3´ †3´-GTCAATCGGAGT<u>GGAXC</u>ACCGTATCGGTCG-5´
S_4	Hemimethylated Targeted CCGG Duplex 　　　　　　　　　　M *5´-TCGAGGCCAGGTAGC<u>CCGG</u>ATCTGGTGGAC-3´ 3´-AGCTCCGGTCCATCG<u>GGCC</u>TAGACCACCTG-5´
S_5	GuaUre-dR Targeted CG Duplex 　　　　　　　　　　M *5´-TCGAGGCCAGGTAGC<u>CCGG</u>ATCTGGTGGAC-3´ †3´-AGCTCCGGTCCATCG<u>GGXC</u>TAGACCACCTG-5´
S_6	GuaUre-dR Targeted CC Duplex 5´-TCGAGGCCAGGTAGC<u>CCCG</u>ATCTGGTGGAC-3´ †3´-AGCTCCGGTCCATCG<u>GGXC</u>TAGACCACCTG-5´

　*M = 2´-Deoxyribo-5-methylcytosine.
　**F = 2´-Deoxyribo-5-fluorocytosine.
　†X = GuaUre-dR.

Phosphate pH = 7, 1 mM EDTA, 7 mM βME) containing 400 mM NaCl, 25 mg/l PMSF. The cells were treated with 30 mg/l of lysozyme for 15 min at 4°C, sonicated 5 times for 1.5 min and centrifuge with type Ti70 rotor at 100 000g at 4°C for 1H. The pooled supernatant was dilute 1.5-fold with Buffer A and loaded into 350 ml of P-11 cellulose column at 2 ml/min. The column was washed with 200 ml of Buffer A with 200 mM NaCl, then linear gradient with 65 ml Buffer A with 200 mM NaCl and 65 ml Buffer A with 800 mM NaCl followed by 500 ml of Buffer A with 800 M NaCl. The fractions containing enzyme were dialyzed overnight against 10 volumes of Buffer A. Dialysate was centrifugated at 10 000g for 15 min in a JA-17 rotor. The supernatant was applied on ÄKTApurifier™ System (GE Healthcare) using 5 ml Hi-Trap DEAE-FF column (0.4 mg protein/ml, GE Healthcare) equilibrated with Buffer A with 50 mM NaCl. The enzyme was eluted with 50 ml linear gradient of 50 mM to 400 mM NaCl in Buffer A. The fractions containing enzyme activity were pooled and applied to a 30 ml of DEAE-Sepharose column at 2.5 ml/min. The column was washed with 150 ml of Buffer A with 50 mM NaCl and the enzyme was eluted within linear gradient of 65 ml Buffer A with 50 mM NaCl and 65 ml Buffer A with

400 mM NaCl. The fractions containing enzyme were pooled together and applied to a hydroxyapatite column (0.12 ml HAP/ml supernatant) equilibrated with buffer A with 200 mM NaCl. The column was washed with 25 ml of Buffer A with 200 mM and the enzyme was eluted with 50 ml of buffer B: 500 mM KPi, 50 mM Tris–Cl pH 7.8, 0.08 mM EDTA, 2.5 mM βME, 25% v/v glycerol. The fractions containing active enzyme were pooled together and concentrated over a second HAP column. Purified enzyme had a specific activity of 92.26 fmol/min/mg.

Microfluidics retardation

The DNA 7500 LabChip (Agilent) was used for the detection of retardation products as previously described (27). Duplex oligodeoxynucleotides, S_0, S_2, S_3 (Table 1) ($c = 2.5 \mu M$) were incubated with *Eco*RII Methyltransferase in 50 mM Tris pH = 7.8, 10 mM EDTA, 5 mM βME with 80 μM cold SAM at 37°C for 2.5 h in 10 μl of the reaction volume.

QPCR: Cycle times, reaction conditions and primer and probe syntheses were as previously described (28). All PCR reactions were carried out on a Rotor Gene 3000 QPCR system (Corbett Life Sciences, Mortlake, NSW Australia). Software provided by the manufacturer was used in data collection and C_t analyses.

QPCR Standards: Cloned plasmid standards were used as previously described (28).

GuaUre-dR preparation

5AzaC-dR (Selleck Chemicals, LLC, Houston, TX, USA) was dissolved with 5% NH₄OH and dried on a SpeedVac® with heating to promote quantitative hydrolytic deformylation of 5azaC-dR and produce pure GuaUre-dR (Supplementary Figure S2). Formation and purity of GuaUre-dR was confirmed by MS [found m/z: 219.00(MH⁺); 436.91(2MH⁺); 654.55(3MH⁺); 872.36(4MH⁺)] (Supplementary Figure S3).

Cell culture, drug treatment and DNA isolation

PC-3 cells were grown at 37°C with humidity and 5% CO₂, in RPMI Medium 1640 (Irvine Scientific, Santa Ana, CA, USA) containing 10% Fetal Bovine Serum and standard antibiotics (10 000 U penicillin and 10 ng/ml streptomycin in 0.9% NaCl; Sigma Aldrich, St Louis, MO, USA). Cells were passaged using 0.25% trypsin EDTA (Gibco, Grand Island, NY, USA), at 1:3 to 1:6. The PC-3 cells were exposed to 5azaC-dR or GuaUre-dR at a concentration of 1 μM. After 48 h, the cells were replenished with fresh media containing fresh drug at the same concentration. Photos of both sets of treated cells were taken using an inverted microscope (Nikon Eclipse TS100) 1, 24, 48 and 72 h after the cells were exposed to the drugs. At each time point after the photos were taken, the cells were counted, trypsinized, and spun at 1000 g for 5 min. The cell pellet was stored at −80°C until DNA extraction and bisulfite treatment. A set of plates with untreated PC-3 cells were also photographed, counted, trypsinized and stored at each time point in order to monitor normal growth and behavior under the same conditions. DNA was isolated from cultured cells using

Qiagen's QIAamp DNA Blood mini kit also as previously described (28).

Cell culture methods and cytotoxicity measurements

For cytotoxicity associated with Fragile Site production, PC-3 cells grown on separate plates were exposed to varying concentrations of GuaUre-dR in duplicate. Another set of plates was left untreated, in order to monitor normal growth and behavior of the PC-3 cells under the same conditions. After the addition of GuaUre-dR, the plates with varying concentrations of GuaUre-dR were incubated for 7 h under the conditions above as a control for fragile site induction and with varying concentrations of GuaUre-dR for 48 h as a control for methylation inhibition. Harvested cells were counted using a hemocytometer, and trypan blue (Sigma Aldrich, St Louis, Missouri, USA) exclusion was used to determine cell viability.

Fragile site induction and cytogenetic analysis

5AzaC-dR or GuaUre-dR was dissolved in nuclease-free water to give 9 mg/ml stock solution. For each experiment, four cultures of the normal cell line RI-EBV, established from lymphocytes from a normal male peripheral blood sample (Karyotype 46XY), grown in RPMI supplemented with 15% FBS, 1% L-glutamine and 1% Pen/Strep were set up and exposed to the drugs at varying concentrations: 10^{-3} M, 10^{-4} M, 10^{-5} M and 0 M. Freshly prepared 5azaC-dR or GuaUre-dR was added to separate 10 ml cell cultures and incubated at 37°C for 7 h. They were exposed to colcemid for 40 min (during the last 40 min of 7 h drug exposure) to inhibit microtubule formation and arrests cells in metaphase. Cells were then harvested by standard methods and slides were prepared. After overnight aging at 60°C, slides were GTG banded and 50 metaphase cells were scored at each drug concentration in each of 2 separate experiments for any evidence of fragility. Each cell was counted and all chromosomes were evaluated for elongation or breaks. Metaphases were captured using Bandview software (Applied Spectral Imaging, Carlsbad, CA, USA).

Bisulfite-mediated PCR

DNA methylation state was determined with the EZ DNA Methylation Kit (Zymo Research, Orange, CA, USA) that was used to treat DNA with bisulfite as previously described (28).

Bisulfite sequencing

Methods used for gel isolation, cloning and sequencing has been have been previously described (29). Briefly, DNA fragments amplified after bisulfite mediated PCR were separated by gel electrophoresis (Figure 4B) and extracted using the QIAquick Gel extraction Kit (Qiagen). Isolated DNA was cloned using the PCR 2.1 TOPO Cloning Kit (Invitrogen) and plasmid DNA containing inserts of the appropriate size were sequenced on an ABI sequencer (Applied Biosystems) by the City of Hope DNA Sequencing Lab.

Adaptor-mediated PCR of deoxyguanylurea-containing oligodeoxynucleotides

The sequences of 30-mer Duplexes S_4, S_5, S_6 are given in Table 1.

Linker_1 (5′-AGAAGCTTGAATTCGAGCAGTCAG-3′) was annealed to linker_2 (5′-CTGCTCGAATTCAAGCTTCT-3′) by adding 2.5 μl of 100 μM of each oligo in 45 μl and incubating them for 2 min at 94°C, 5 min at 70°C and for 5 min at 50°C, then the duplex was allowed to cool to room temperature. The duplex was diluted to a final volume of 250 μl for a 1 μM duplex linker. 500 pmol of each 30-mer Duplex was phosphorylated with 10 U of T4 PNK (NEB) in 1 × ligation buffer (NEB). Two microliters of each phosphorylated oligo was added to 10 μl of TE pH 7.5 and annealed under the same temperature conditions as the linkers. Then, 1μl of phosphorylated annealed 30-mer duplex was ligated to 1 μl 1 μM linker with 5 U of T4 ligase (NEB), in 1 × ligation buffer (NEB) in a final volume of 15 μl. This was incubated overnight at 4°C. The ligated DNA was then treated with the Qiagen reaction cleanup kit, and the DNA was eluted in 15 μl of pure water. The eluted DNA was used for PCR, with 0.25 U of Hotstar Taq (Qiagen), 10 μl of 10 × Taq Buffer (Qiagen), 8 μl 25 mM $MgCl_2$, 1.6 μl of 10 mM dNTPs (Roche), 1 μl 100 μM linker 2 in a final volume of 100 μL. The PCR conditions were 55°C 2 min, 72°C 5 min, 94°C 10 min, 24 cycles of 94°C 1 min, 55°C 1 min, 72°C 1 min and then 72°C for 5 min, with a 4°C hold. Then 4 μl of the PCR reaction was cloned using the TOPO-TA cloning kit (Invitrogen) following the manufacturer's instructions. Plasmids with inserts of the appropriate size were sequenced at the City of Hope DNA Sequencing Lab as previously described (30).

Detection of mutations at the APC locus

The following primers were used for mutation analysis at the APC locus: forward 5′-ACTGCCATCAACTTCCTTGC-3′ and reverse 5′-ACCTACCCCATTTCCGAGTC-3′. APC gene sequences from the untreated PC3 DNA and from PC3 DNA treated with 5-azacytidine or deoxyguanylurea were amplified through 50 cycles of: 95°C for 15 s, 56°C for 30 s, 72°C for 30 s. The band corresponding to the 318 bp product was gel-extracted using the QIAquick gel extraction kit (Qiagen, Valencia, CA, USA). Once isolated, 4 μl of the Eluted Gel extract was used for cloning with the TOPO-TA cloning kit (Invitrogen), as described by the manufacturer. The resulting colonies were inoculated into liquid cultures and plasmid DNA was isolated from each. Plasmids with inserts of the appropriate size were sequenced at the City of Hope DNA Sequencing Lab as previously described (30).

Melting temperatures for GuaUre-modified duplexes

The 5 μg of each duplex DNA (Supplementary Table S1) were annealed and subjected to high resolution melting on a Rotor Gene R-6000 QPCR system (Qiagen) in a volume of 25 μl of buffer containing: 0.06 U of Hotstar Taq (Qiagen), 2.5 μl of 10 × Taq Buffer (Qiagen), 2 μl 25 mM $MgCl_2$, using SYTO® 9 (Invitrogen™) as a fluorescent

stain. The melt cycle conditions were: 95°C 6 min, 72°C 10 min, 56°C 10 min, 25°C 10 min, melt from 66°C to 99°C.

RESULTS

Effects of the breakdown product in DNA

We suspected that GuaUre-dR itself might account for the inhibition of DNA methyltransferase. To test this idea, we prepared the NPE, NPEOC-GuaUre-dR phosphoramidite (Figure 1), high-yield syntheses of single-stranded oligodeoxynucleotides containing GuaUre-dR were easily achieved with the NPE, NPEOC-GuaUre-dR phosphoramidite and corresponding NPE, NPEOC-phosphoramidites of the other bases.

Inhibition of bacterial DNA methyltransferase (M.*Eco*RII) and human DNA methyltransferase I by DNA containing GuaUre-dR

Purified M.*Eco*RII was dramatically inhibited by GuaUre-dR in duplex S_3 at the targeted cytosine in its CCWGG recognition site (Figure 2A), while hDNMT1 was dramatically inhibited by GuaUre-dR at the targeted C in a CG recognition site in duplex S_5 (Figure 2B) or at a mispair in a non-CG site in duplex S_6 (Figure 2C). The inhibition kinetics for each enzyme were best fit by competition between the productive substrate with dC targeted by the methyltransferase and the non-productive substrate with GuaUre-dR targeted by the enzyme. Figure 2 shows the kinetics of the methyltransferase reaction when either dC or GuaUre-dR is targeted by a symmetrically placed 5-methylcytosine residue in hemimethylated DNA. Kinetic parameters for the hemimethylated reaction targeting dC are easily determined from the saturation plot for that substrate. However, the hemimethylated reaction targeting GuaUre-dR is very slow, making exact determination of the Km for the GuaUre-dR targeted substrate uncertain. To obtain kinetic parameters for this substrate, reaction rates were determined for a fixed concentration of the hemimethylated dC targeted substrate in the presence of varying amounts of hemimethylated GuaUre-dR targeted substrate. The kinetics are described by the following rate equation (31):

$$v = \frac{\frac{V_m^{dC}[S_{dC}]}{K_m^{dC}} + \frac{V_m^{GuaUredR}[S_{GuaUredR}]}{K_m^{GuaUredR}}}{1 + \frac{[S_{dC}]}{K_m^{dC}} + \frac{[S_{GuaUredR}]}{K_m^{GuaUredR}}} \tag{1}$$

When the data for M.*Eco*RII are fit to this equation using V_m^{dC}, $V_m^{GuaUredR}$ and K_m^{dC} determined from the standard saturation plots (not shown), the upper bound for $K_m^{GuaUredR}$ is found to be 6.7 ± 5.3 nM at 67% confidence. Since K_m^{dC} is 624 nM and V_m^{dC} is 244 fmol/min, the enzyme binds about 90 times more tightly to the GuaUre-dR substrate in a very much less productive complex with a $V_m^{GuaUredR}$ of only 2.6 fmol/min.

We performed the same kinetic analysis with hDNMT1 with similar results. Using V_m^{dC}, $V_m^{GuaUredR}$ and K_m^{dC} determined from the standard saturation plots (not shown),
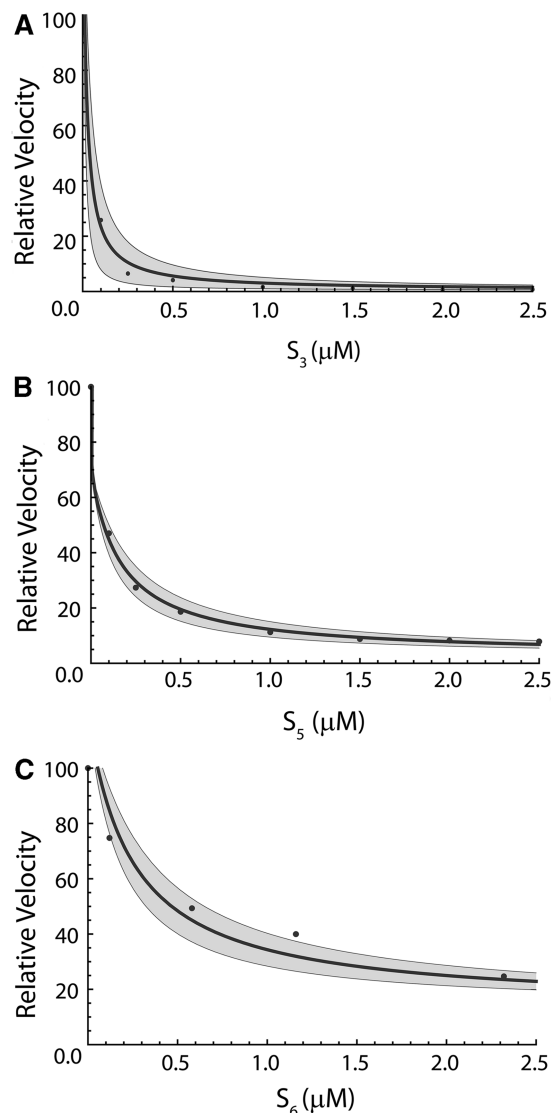
Figure 2. Inhibition of DNA methyltransferases by 2′-deoxyguanyl urea-containing oligodeoxynucleotides. Hemimethylated duplexes S_1, S_4 (Table 1) containing the three-nucleotide recognition sequence of the human enzyme are rapidly methylated at the methyl-directed target cytosine in the CG site on the opposite strand. (**A**) For a representative bacterial methyltransferase (M.*Eco*RII), maximal incorporation (576.03 fmol/min = 100%) was achieved with duplex S_1 alone. When a duplex S_3 carrying GuaUre-dR at the targeted base (indicated with an X in the sequences in Table 1) was added at the indicated concentrations, the reaction was strongly inhibited. (**B**) For a human DNA methyltransferase 1 maximal incorporation (99.58 fmol/min = 100%) was achieved with duplex S_4 alone. When duplex S_5 carrying a GuaUre-dR at the targeted C in a CG recognition site was added at the indicated concentrations, the reaction was strongly inhibited. (**C**) For a human DNA methyltransferase 1 maximal incorporation (99.58 fmol/min = 100%) was achieved with duplex S_4 alone. When duplex S_6 carrying GuaUre-dR at a mispair in a non-CG was added to the reaction at the indicated concentrations, the reaction was strongly inhibited.

the upper bound for $K_m^{GuaUredR}$ is found to be 42 ± 14 nM at 67% confidence from equation 1. Since K_m^{dC} is 323 nM and V_m^{dC} is 93 fmol/min, the enzyme binds about 8 times more tightly to the GuaUre-dR substrate in

a very much less productive complex with a $V_m^{GuaUredR}$ of only 2.3 fmol/min.

Microfluidics retardation of DNA methyltransferase by GuaUre-containing oligodeoxynucleotides

The kinetic data above strongly suggests that DNA methyltransferase binds tightly GuaUre containing oligodeoxynucleotides. To further support this inference, we performed microfluidics retardation experiments with GuaUre-dR containing oligodeoxynucleotides (Figure 3). In this experiment, the GuaUre-dR targeted duplex S_3 was found to be retarded by M.*Eco*RII to the same extent as the control 5FdC targeted duplex S_2 known to tightly bind DNA methyltransferases (27). Binding with GuaUre-dR appeared somewhat less effective than binding to 5FdC, suggesting that the enzyme may select only one of the solution conformations adopted by GuaUre-dR.

Demethylation of human DNA by GuaUre-dR

Unlike 5azaC-R (32) and 5azaC-dR, GuaUre-dR did not appear to have an effect on bacterial growth (not shown), however, we noted that both of 5azaC-dR and GuaUre-dR were strong inhibitors of the growth of human prostate cancer cells. Moreover, both compounds effectively inhibited DNA methylation at genes inspected by methylation sensitive PCR. The time course of demethylation at a representative promoter is depicted in Figure 4.

Induction of 5AzaC-dR type fragile sites by GuaUre-dR

Experiments comparing the pattern of fragile site induction by 5azaC-dR (Figure 5B) and GuaUre-dR (Figure 5C) with untreated normal cells (Figure 5A) demonstrate that the well-known fragile sites FRA1J and FRA9F (7) are induced by either compound administered at identical concentrations. The results of two independent experiments were quantified by determining the number of metaphases out of the 50 examined that contained fragile sites (Table 2). In terms of the total number of fragile sites observed (0 observed in 100 total metaphases with GuaUre-dR compared to 4 in 100 metaphases for 5azaC-dR at 10^{-5} M and 32 observed in 100 total metaphases with GuaUre-dR compared to 10 in 100 metaphases for 5azaC-dR at 10^{-3} M) the breakdown product appears to be less effective at fragile site induction than 5azaC-dR at low concentration and more effective at higher concentration.

Cytotoxicity of a representative prostate cancer cell line

As has been noted for 5azaC-dR, GuaUre-dR exhibits minimal toxicity to prostate cancer cells at low concentration (Figure 6). With GuaUre-dR, cytotoxicity depended on time of exposure. Essentially no cytotoxicity was observed with the drug over the range zero to 1 mM after 7 h of exposure used in detection of fragile sites. However, after 48 h of exposure, used in the detection of DNA methylation change significant cytotoxicity was observed at 0.5 μM with an apparent LD50 of ~48 μM.
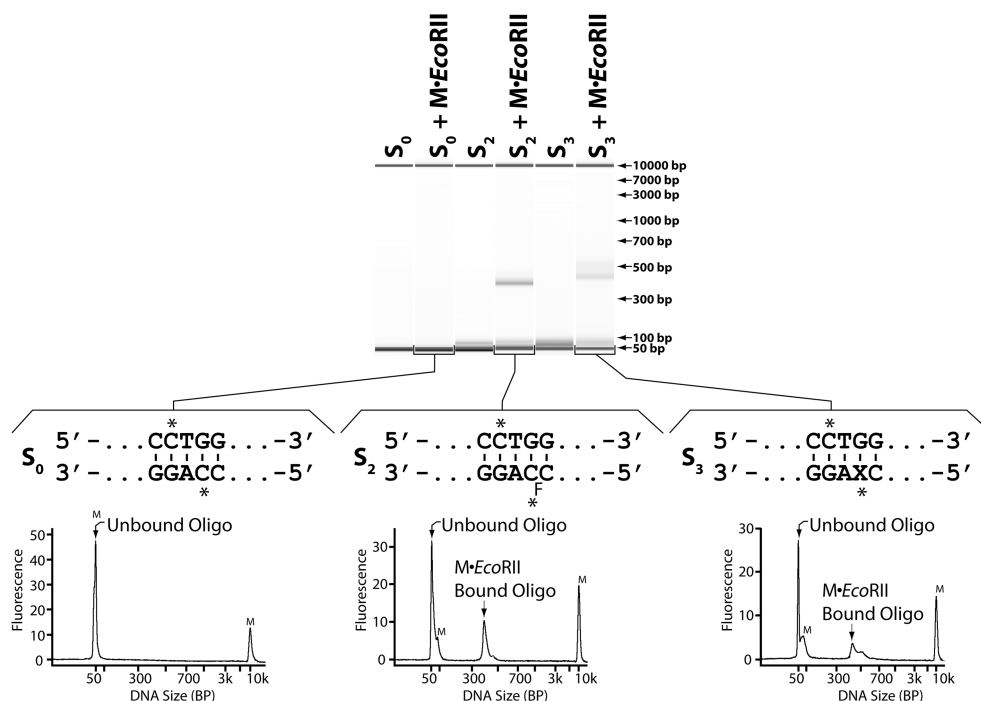

Figure 3. Microfluidics retardation of DNA methyltransferase by GuaUre-dR-containing DNA. The microfluidics data are presented as a gel separation pattern (Top). Lane scans for the lanes containing DNA methyltransferase are presented at the bottom of the figure. The FdC Targeted CCWGG duplex S_2 was used as an M.*Eco*RII binding reference. The GuaUre-dR targeted CCWGG duplex S_3 gave a comparable retardation pattern, while the control *de novo* CCWGG duplex S_0 was not retarded.
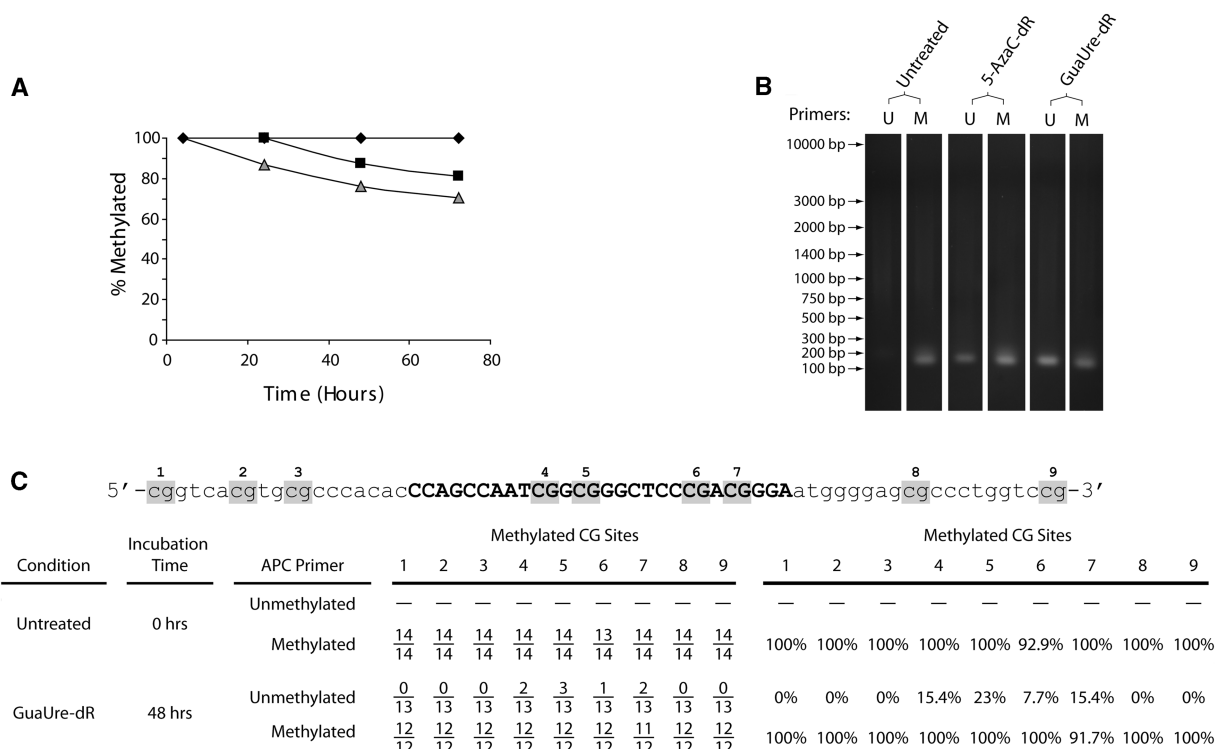
A

B

C

```
                1        2   3                          4    5         6   7                       8            9
5'-cggtcacgtgcgcccacacCCAGCCAATCGGCGGGCTCCCGACGGGAatggggagcgccctggtccg-3'
```

Condition	Incubation Time	APC Primer	Methylated CG Sites									Methylated CG Sites								
			1	2	3	4	5	6	7	8	9	1	2	3	4	5	6	7	8	9
Untreated	0 hrs	Unmethylated	—	—	—	—	—	—	—	—	—	—	—	—	—	—	—	—	—	—
		Methylated	$\frac{14}{14}$	$\frac{14}{14}$	$\frac{14}{14}$	$\frac{14}{14}$	$\frac{14}{14}$	$\frac{13}{14}$	$\frac{14}{14}$	$\frac{14}{14}$	$\frac{14}{14}$	100%	100%	100%	100%	100%	92.9%	100%	100%	100%
GuaUre-dR	48 hrs	Unmethylated	$\frac{0}{13}$	$\frac{0}{13}$	$\frac{0}{13}$	$\frac{2}{13}$	$\frac{3}{13}$	$\frac{1}{13}$	$\frac{2}{13}$	$\frac{0}{13}$	$\frac{0}{13}$	0%	0%	0%	15.4%	23%	7.7%	15.4%	0%	0%
		Methylated	$\frac{12}{12}$	$\frac{12}{12}$	$\frac{12}{12}$	$\frac{12}{12}$	$\frac{12}{12}$	$\frac{11}{12}$	$\frac{12}{12}$	$\frac{12}{12}$	$\frac{12}{12}$	100%	100%	100%	100%	100%	100%	91.7%	100%	100%

Figure 4. Demethylation at the human APC promoter. (**A**) Time course of demethylation at the human APC promoter by 5azaC-dR or GuaUre-dR. Filled diamonds, no treatment; filled squares, 1 μM 5azaC-dR; filled triangles, 1 μM GuaUre-dR. (**B**) Electrophoretic separation of methylation sensitive PCR amplification products after 48 h exposure to 1 μM GuaUre-dR. (**C**) Methylation levels at CG sites determined by bisulfite sequencing (see also Supplementary Figure S4). CG sites 1, 2, 3 and 8 and 9 are contained in the methylation sensitive PCR primers (lower case). CG sites 4, 5, 6 and 7 are in the amplified region (uppercase, bold).

Mutagenesis by GuaUre-dR

GuaUre-dR created by direct incorporation or by the incorporation and subsequent breakdown of 5azaC-dR is expected to produce transversion mutations based the ability of GuaUre-dR to pair with dC (10). Consequently, GuaUre-dR incorporated directly into DNA as a dG analog would be expected to be essentially non-mutagenic. We used PCR amplification of synthetic duplex oligodeoxyynucleotides containing GuaUre-dR at preselected sites to infer probable replication base pairing at template sites containing GuaUre-dR (Figure 7). Based on this analysis the base pairing frequencies for GuaUre-dR were GuaUre-dR:dG ≫ GuaUre-dR:dA > GuaUre-dR:-dC, suggesting that Taq polymerase codes GuaUre-dR primarily as a dC analog during PCR amplification. It should be noted that in this analysis oligodeoxynucleotides are expected to form tandem arrays after ligation in the ligation mediated PCR procedure. The clones isolated from oligodeoxynucleotides containing GuaUre-dR on only one of the two strands in the duplex generally contained tandem arrays of 2–5 copies of the oligodeoxynucleotide. However, tandem arrays were not observed when the input oligodeoxynucleotide contained GuaUre-dR on both strands. This clearly suggests that GuaUre-dR is a replication block to the Taq polymerase.

Since GuaUre-dR was found to be an effective demethylating agent in human cells, we tested a representative gene for the presence of mutations after demethylation by GuaUre-dR. When a short (318 bp) region of the APC gene in PC3 cells was inspected after growth in GuaUre-dR containing medium, a significant number of transition, transversion, deletion and insertion mutations were detected (Figure 8).

DISCUSSION

Many studies have demonstrated that 5azaC-R and 5azaC-dR are unstable in aqueous solution (13,33,34), however, studies on the stability 5azaC-dR in DNA have not been reported. The intrinsic stability of cytosine in B-DNA can be attributed largely to the activation energy associated with the formation of the dihydrocytosine intermediate required for hydrolytic deamination. In that case two sp3 carbons must be introduced into the cytosine ring forcing a dramatic disruption of the structure of the DNA double helix that is resisted by the stacking energy of the duplex. Low levels of cytosine hydrate formed in aqueous solution are expected. However, restoration of the cytosine ring by ß-elimination is favored by the stacking energy, hence cytosine deamination mutations are rare. In contrast, the dihydroazacytidine intermediate can form more easily than dihydrocytidine intermediate because C6 is more electrophilic in the triazine ring and because the deformation of the ring is less pronounced because only one sp3
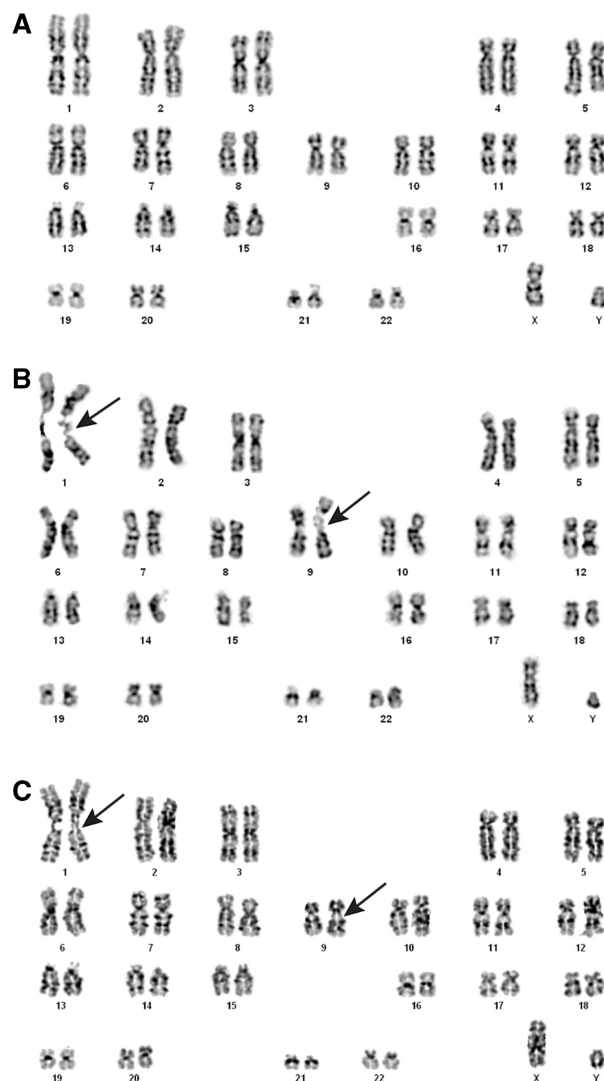
Figure 5. Induction of fragile sites, FRA1J [fra(1)(q12)] and FRA9F [fra (9)(q12)] (black arrows). (**A**) No treatment karyotype, (**B**) 5azaC-dR (10^{-3} M) or (**C**) GuaUre-dR (10^{-3} M) in a normal male cell line. Five out of 100 metaphases contained affected sites with 5azaC-dR at 10^{-3} M. Sixteen out of 100 metaphases had affected sites with GuaUre-dR at 10^{-3} M.

carbon is formed as N5 remains essentially planar. Further, once formed the dihydroazacytidine intermediate is unstable and rapidly breaks down to the guanylurea restoring the planar system in duplex DNA. Essentially, the electrophilicity of 5azaC-dR in DNA can be viewed as driving nucleophilic attack and the stacking energy of the duplex can be viewed as driving the breakdown of the dihydroazacytidine intermediate. Consequently, 5azaC is expected to be intrinsically unstable in DNA. In short, the chemistry of the triazine ring in DNA strongly suggests that direct incorporation of 5azaC-dR in DNA will rapidly result in the production of GuaUre-dR at sites of incorporation, and that GuaUre-dR incorporated directly into DNA would produce the same end result: GuaUre-dR in DNA.

This hypothesis is supported not only by the data presented here, but also by the literature on 5azaC action.

For example, the spectrum of mutations produced by 5azaC-dR in treated mice includes C:G → T:A transitions, C:G → A:T transversions and an excess of C:G → G:C transversions at the d(CG) site (10). One possible explanation for the excess of C:G → G:C transversions is that DNMT1 attacks 5azaC-dR in DNA followed by hydrolysis within the active site of the enzyme to produce formylated DNMT1 and GuaUre-dR at the CG site (10), allowing GuaUre-dR thus formed to code for dC at replication. Several lines of evidence argue against this model. First, the active site of DNMT1 is essentially impervious to water as demonstrated by the complete lack of cytosine deamination during catalytic methylation (35). Consequently, anhydrous nucleophilic attack at C6 by the active site cysteine is expected to produce C6-DNMT dihydroazacytidine in equilibrium with a ring-open covalent intermediate (see Supplementary Figure S1). Second, substitution of the weaker serine nucleophile for the cysteine at the active site of DNMT1 does not block its subsequent enzyme degradation (12). Third, the model does not account for the significant number of C:G → T:A transitions and C:G → A:T transversions that are detected after mutagenesis by 5azaC-dR (10). Fourth, in bacteria C:G → A:T transversions and C:G → G:C transversions are preferentially selected after 5azaC-R mutagenesis in the absence of methytransferase interaction (1).

Given the tight binding of DNMT1 at sites of GuaUre-dR substitution inferred from the kinetics of DNMT1 inhibition by GuaUre-dR, the degradation of the enzyme is more likely associated with the removal of tight complexes formed with GuaUre-dR as has been observed with tight complexes formed between the DNMT1 and 2-pyrimidinone (36,37). The predominance of transversions *in vivo* would then be associated with either the removal of GuaUre-dR by DNA glycosylases or the formation of abasic sites followed by the incorporation of dA by bypass synthesis, or the mispairing of GuaUre-dR with dA (Figure 7).

The mutational spectrum obtained after PCR amplification of GuaUre-dR containing oligodeoxynucleotides measures base pairing propensities in the absence of repair since Taq polymerase lacks both exonuclease and glycosylase activities. That evidence clearly shows that copying by Taq polymerase favors GuaUre-dR:dG paring and not GuaUre-dR:dC paring during amplification. Given that the ΔTm for each of these ring-open conformations relative to the dC:dG pair is comparable (Supplementary Table S1), we infer that the GuaUre-dR:dG base pair is preferred because it most closely approximates the geometry of the dC:dG basepair (38). The *in vivo* mutational spectrum at the APC gene after exposure to GuaUre-dR strongly suggests that it is highly mutagenic. Transversions and deletions were produced at an aggregate frequency of 1.56×10^{-3}/bp while transition mutations were detected at a lower aggregate frequency 0.39×10^{-3}/bp, suggesting that mutations generated by abasic sites formed after base excision are more prevalent than mispairing mutations in human cells.

Although the base-pairing properties of GuaUre-dR provide the best explanation for the observed mutagenesis

Table 2. Induction of 5-azacytidine-type chromosomal fragile sites by GuaUre-dR in the RI-EBV cell line

Conc.	Experiment	5azaC-dR		GuaUre-dR	
		Abnormal metaphases[a]	Abnormal karyotypes	Abnormal metaphases	Abnormal karyotypes
0 M	1	0/50	——	0/50	——
	2	0/50	——	0/50	——
10^{-5} M	1	0/50	None	0/50	None
	2	2/50 (4 sites)	46,XY,fra(1)(q12)x2 [2 cells]	0/50	None
10^{-4} M	1	5/50 (5 sites)	46,XY,fra(1)(q24) [2 cells, 2 sites] 46,XY,fra(9)(q12) [2 cells, 2 sites] 46,XY,fra(1)(q12) [1 cell, 1 site]	4/50 (4 sites)	46,XY,fra(1)(q12) [2 cells, 2 sites] 46,XY,chrb (4) [2 cells, 2 sites]
	2	2/50 (3 sites)	46,XY,fra(1)(q12)x1 [1 cell,1 site] 46,XY,fra(1)(q12)x2 [1 cell, 2 sites]	3/50 (6 sites)	46,XY,fra(1)(q12), fra(9)(q12)[2 cells, 4 sites] 46,XY,fra(1)(q12)x2 [1 cell, 2sites]
10^{-3} M	1	2/50 (5 sites)	46,XY,fra(1)(q12)x2,fra(9)(q12) [1 cell, 3 sites] 46,XY,fra(1)(q12)x2 [1 cell, 2 sites]	11/50 (23 sites)	46,XY,fra(1)(q12)x2,fra(9)(q12) [6 cells, 18 sites] 46,XY,fra(1)(q12) [5 cells, 5 sites]
	2	3/50 (5 sites)	46,XY,fra(1)(q12)x2 [1 cell, 2 sites] 46,XY,fra(1)(q12)x1 [1 cell, 1 site] 46,XY,fra(1)(q12), fra(9)(q12) [1 cell, 2 sites]	5/50 (9 sites)	46,XY,fra(1)(q12), fra(9)(q12)[2 cells. 4 sites] 46,XY,fra(1)(q12)x2 fra(9)(q12) [1 cell, 3 sites] 46,XY,fra(1)(q12)x1 [2 cells, 2 sites]

[a]Number abnormal metaphases observed in 50 examined per experiment followed by the number of fragile sites present in parentheses.
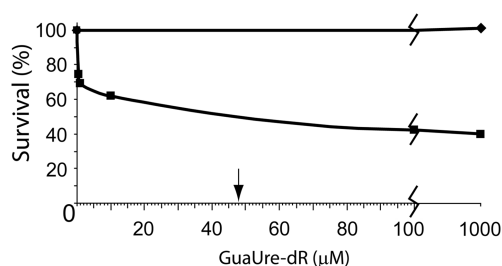

Figure 6. Limited cytotoxicity of GuaUre-dR in the PC3 cell line. Cellular viability is plotted as a function of GuaUre-dR concentration, after 7 h [filled dashed diamonds] or 48 h [filled dashed squares] of exposure to the drug. The apparent LD50 after 48 h of exposure is marked with an arrow.

by 5azaC-R in both bacteria (1) and mammals (10), as a ring-open base, it may not be a particularly good substrate for direct incorporation into DNA by mammalian DNA polymerases. However, direct incorporation of GuaUre-dR is again made plausible by the ability of this drug to induce the 5-azacytidine-type chromosomal fragile sites: FRA1J and FRA9E (Figure 5, Table 2). These fragile sites have hitherto been uniquely associated the induction by 5azaC-R or 5azaC-dR. The possibility that GuaUre-dR is directly incorporated into DNA is supported by the similarity between fragile sites FRA1J and FRA9E and the 1qh and 9qh undercondensations often observed in ICF syndrome (39). Since ICF syndrome is caused by mutations in human DNMT3b it is reasonable to suspect that GuaUre-dR and 5azaC-dR are incorporated into DNA where they inhibit DNMT3b directly. However, the present data does not directly demonstrate incorporation into DNA. Consequently, it remains possible that these drugs merely block a process involved in chromosome condensation that requires DNMT3b activity. In any event, the data reported here

clearly demonstrates that induction of these fragile sites is not unique to 5azaC-dR, and suggests that induction of fragile sites by GuaUre-dR, like 5azaC-dR induced mutagenesis, is the result of its breakdown to GuaUre-dR, which can occur rapidly. In general, cell lines are treated with 5azaC-R or 5azaC-dR for between 3 and 5 days (40,41). During that time the concentration of either compound will decrease from 1 μM usually used to 1 nM while the concentration of GuaUre-R or GuaUre-dR will increase correspondingly to about 1 μM (13,33).

Earlier work (42) showed no therapeutic benefit for GuaUre-R in an L1210 mouse tumor model. Given that the mammalian cytidine kinase is quite promiscuous (43) phosphorylation of either GuaUre-R or GuaUre-dR should be effective in mammalian cells. This suggests that the inability of GuaUre-R to kill L1210 cells in a mouse model (43) may reside in the inability of ribnucleotide reductase to convert the monophosphate GuaUre-RMP to GuaUre-dRMP. This is consistent with the relatively low LD50 associated with GuaUre-dR in PC3 prostate tumor cells, and with more recent studies showing that epigenetic therapy with 5azaC-dR alone was only moderately effective against solid tumor cells (44). Durable responses in solid tumors appear to require low doses of methyltransferase inhibitors in combination with histone deacetylase inhibitors followed by a course of cytotoxic therapy (45), suggesting that epigenetic alterations induced by these drugs may sensitize tumors to subsequent cytotoxic thereapy. In any event, for a rapidly dividing cell culture, one can expect ∼10–20% of the input 5azaC-dR to be incorporated into DNA where it will spontaneously hydrolyze to GuaUre-dR.

Ultimately our results coupled with the results of Ghoshal *et al.* (12) suggest that GuaUre-dR is directly incorporated into DNA and/or created by hydrolysis of 5azaC-dR in DNA. The resulting massive and random conversion of dG:dC base pairs to GuaUre-dR:dG or

PCR Target Sequence	Amplicon Sequence	30-mer Clone Count	Site Count	Implied Base Paring
5'-CXGG-3' 3'-GGXC-5'	5'-CCGG-3' 3'-GGCC-5'	11/15		
5'-CXGG-3' 3'-GGXC-5'	5'-CGGG-3' 3'-GCCC-5'	1/15	26/30	
5'-CXGG-3' 3'-GGXC-5'	5'-CCAG-3' 3'-GGTC-5'	3/15		GuaUre-dR dG
5'-CCCG-3' 3'-GGXC-5'	5'-CCGG-3' 3'-GGCC-5'	1/9	1/9	
5'-CCGG-3' 3'-GGXC-5'	5'-CCGG-3' 3'-GGCC-5'	20/22	20/22	
5'-CXGG-3' 3'-GGXC-5'	5'-CCAG-3' 3'-GGTC-5'	3/15	3/30	
5'-CCGG-3' 3'-GGXC-5'	5'-CCAG-3' 3'-GGTC-5'	2/22	2/22	GuaUre-dR dA
5'-CXGG-3' 3'-GGXC-5'	5'-CGGG-3' 3'-GCCC-5'	1/15	1/30	
5'-CCCG-3' 3'-GGXC-5'	5'-CCCG-3' 3'-GGGC-5'	8/9	8/9	GuaUre-dR dC

Figure 7. Base-pairing preferences inferred from PCR-amplified oligodeoxynucleotides. PCR amplification of ligated oligodeoxynucleotides carrying GuaUre-dR at the indicated sites (X) yielded the sequence substitutions shown. The inferred base-paring schemes are indicated to the right of the figure. Tandem arrays of 30 bp oligos were observed in the cloned product when GuaUre-dR was present on only one strand of the synthetic duplex 30-mer, however, arrays were not observed among the clones with GuaUre-dR present on both strands. Clone count refers to the number of 30mers recovered with the stated sequence alteration. Three different sequences were studied, one sequence gave 22 clones, one gave 15 clones and the third gave 9 clones.

Figure 8. Human mutation frequencies within the APC gene. A variety of mutations were induced in human PC3 cells exposed to GuaUre-dR. In this 318 bp segment of the APC gene, transversions $C:G \rightarrow G:C$ 7.8×10^{-4} bp, transitions $A:T \rightarrow G:C$ 3.9×10^{-4} bp, deletions ΔG 3.9×10^{-4} bp ΔC 3.9×10^{-4} bp and insertion mutations $\hat{} \rightarrow A$ 3.9×10^{-4} bp were observed.

GuaUre-dR:dC basepairs is expected to result in tightly bound methyltransferases, of which the primary maintenace methyltransferase (DNMT1) appears to be uniquely subject to ubiquitination and subsequent proteolytic degradation (12). Moreover, since tight binding to mispairs in a variety of contexts is a fundamental property of DNMT1 this mechanism is consistent with a stoichiometric role for DNMT1 in mammalian DNA

repair (25,46,47). Finally our results suggest that dosage in the therapeutic use of 5azaC-dR (dicitabine) (48–50) could be better controlled by the use of GuaUre-dR.

SUPPLEMENTARY DATA

Supplementary Data are available at NAR Online: Supplementary Table 1 and Supplementary Figures 1–4.

ACKNOWLEDGEMENTS

FUNDING

REFERENCES

1. Cupples,C.G. and Miller,J.H. (1989) A set of lacZ mutations in Escherichia coli that allow rapid detection of each of the six base substitutions. *Proc. Natl Acad. Sci. USA*, **86**, 5345–5349.
2. Fucik,V., Zadrazil,S., Sormova,Z. and F.S. (1965) Mutagenic effects of 5-azacytidine in bacteria. *Collect. Czech. Chem. Commun.*, **30**, 2883–2886.
3. Bhagwat,A.S. and Roberts,R.J. (1987) Genetic analysis of the 5-azacytidine sensitivity of Escherichia coli K-12. *J. Bacteriol.*, **169**, 1537–1546.
4. Call,K.M., Jensen,J.C., Liber,H.L. and Thilly,W.G. (1986) Studies of mutagenicity and clastogenicity of 5-azacytidine in human lymphoblasts and Salmonella typhimurium. *Mutat. Res.*, **160**, 249–257.
5. Carr,B.I., Reilly,J.G., Smith,S.S., Winberg,C. and Riggs,A. (1984) The tumorigenicity of 5-azacytidine in the male Fischer rat. *Carcinogenesis*, **5**, 1583–1590.
6. Harris,M. (1982) Induction of thymidine kinase in enzyme-deficient Chinese hamster cells. *Cell*, **29**, 483–492.
7. Schmid,M., Haaf,T. and Grunert,D. (1984) 5-Azacytidine-induced undercondensations in human chromosomes. *Hum. Genet.*, **67**, 257–263.
8. Hori,T.A. (1983) Induction of chromosome decondensation, sister-chromatid exchanges and endoreduplications by 5-azacytidine, an inhibitor of DNA methylation. *Mutat. Res.*, **121**, 47–52.
9. Komashko,V.M. and Farnham,P.J. (2010) 5-azacytidine treatment reorganizes genomic histone modification patterns. *Epigenetics*, **5**, 229–240.
10. Jackson-Grusby,L., Laird,P.W., Magge,S.N., Moeller,B.J. and Jaenisch,R. (1997) Mutagenicity of 5-aza-2′-deoxycytidine is mediated by the mammalian DNA methyltransferase. *Proc. Natl Acad. Sci. USA*, **94**, 4681–4685.
11. Juttermann,R., Li,E. and Jaenisch,R. (1994) Toxicity of 5-aza-2′-deoxycytidine to mammalian cells is mediated primarily by covalent trapping of DNA methyltransferase rather than DNA demethylation. *Proc. Natl Acad. Sci. USA*, **91**, 11797–11801.
12. Ghoshal,K., Datta,J., Majumder,S., Bai,S., Kutay,H., Motiwala,T. and Jacob,S.T. (2005) 5-Aza-deoxycytidine induces selective degradation of DNA methyltransferase 1 by a proteasomal pathway that requires the KEN box, bromo-adjacent

13. Rogstad,D.K., Herring,J.L., Theruvathu,J.A., Burdzy,A., Perry,C.C., Neidigh,J.W. and Sowers,L.C. (2009) Chemical decomposition of 5-aza-2′-deoxycytidine (Decitabine): kinetic analyses and identification of products by NMR, HPLC, and mass spectrometry. *Chem. Res. Toxicol.*, **22**, 1194–1204.
14. Jones,P.A. and Taylor,S.M. (1980) Cellular differentiation, cytidine analogs and DNA methylation. *Cell*, **20**, 85–93.
15. Christman,J.K., Schneiderman,N. and Acs,G. (1985) Formation of highly stable complexes between 5-azacytosine-substituted DNA and specific non-histone nuclear proteins. Implications for 5-azacytidine-mediated effects on DNA methylation and gene expression. *J. Biol. Chem.*, **260**, 4059–4068.
16. Friedman,S. (1982) Bactericidal effect of 5-azacytidine on Escherichia coli carrying EcoRII restriction-modification enzymes. *J. Bacteriol.*, **151**, 262–268.
17. Pfleiderer,W. (2007) Universal 2-(4-nitrophenyl)ethyl and 2-(4-nitrophenyl)ethoxycarbonyl protecting groups for nucleosides and nucleotides. *Curr. Protoc. Nucleic Acid Chem.*, Chapter 2, Unit 2 13.
18. Guimil Garcia,R., Brank,A.S., Christman,J.K., Marquez,V.E. and Eritja,R. (2001) Synthesis of oligonucleotide inhibitors of DNA (Cytosine-C5) methyltransferase containing 5-azacytosine residues at specific sites. *Antisense Nucleic Acid Drug Dev.*, **11**, 369–378.
19. Liu,M.C., Luo,M.Z., Mozdziesz,D.E., Lin,T.S., Dutschman,G.E., Cheng,Y.C. and Sartorelli,A.C. (1999) Synthesis of 2′-methylene-substituted 5-azapyrimidine, 6-azapyrimidine, and 3-deazaguanine nucleoside analogues as potential antitumor/antiviral agents. *Nucleosides Nucleotides*, **18**, 55–72.
20. Diaz,A.R., Eritjaa,R. and Garcia,R.G. (1997) Synthesis of oligodeoxynucleotides containing 2-substituted guanine derivatives using 2-fluoro-2′-deoxyinosine as common nucleoside precursor. *Nucleosides, Nucleotides Nucleic Acids*, **16**, 2035–2051.
21. Alul,R.H., Singman,C.N., Zhang,G.R. and Letsinger,R.L. (1991) Oxalyl-CPG: a labile support for synthesis of sensitive oligonucleotide derivatives. *Nucleic Acids Res.*, **19**, 1527–1532.
22. Pon,R.T. and Yu,S. (1997) Hydroquinone-O,O′-diacetic acid ('Q-linker') as a replacement for succinyl and oxalyl linker arms in solid phase oligonucleotide synthesis. *Nucleic Acids Res.*, **25**, 3629–3635.
23. Dignam,J.D., Lebovitz,R.M. and Roeder,R.G. (1983) Accurate transcription initiation by RNA polymerase II in a soluble extract from isolated mammalian nuclei. *Nucleic Acids Res.*, **11**, 1475–1489.
24. Okuwaki,M. and Verreault,A. (2004) Maintenance DNA methylation of nucleosome core particles. *J. Biol. Chem.*, **279**, 2904–2912.
25. Kho,M.R., Baker,D.J., Laayoun,A. and Smith,S.S. (1998) Stalling of human DNA (cytosine-5) methyltransferase at single-strand conformers from a site of dynamic mutation. *J. Mol. Biol.*, **275**, 67–79.
26. Friedman,S. (1985) The irreversible binding of azacytosine-containing DNA fragments to bacterial DNA(cytosine-5)methyltransferases. *J. Biol. Chem.*, **260**, 5698–5705.
27. Clark,J., Shevchuk,T., Swiderski,P.M., Dabur,R., Crocitto,L.E., Buryanov,Y.I. and Smith,S.S. (2003) Mobility-shift analysis with microfluidics chips. *Biotechniques*, **35**, 548–554.
28. Munson,K., Clark,J., Lamparska-Kupsik,K. and Smith,S.S. (2007) Recovery of bisulfite-converted genomic sequences in the methylation-sensitive QPCR. *Nucleic Acids Res.*, **35**, 2893–2903.
29. Clark,J. and Smith,S.S. (2008) Secondary structure at a hot spot for DNA methylation in DNA from human breast cancers. *Cancer Genomics Proteomics*, **5**, 241–251.
30. Shevchuk,T., Kretzner,L., Munson,K., Axume,J., Clark,J., Dyachenko,O.V., Caudill,M., Buryanov,Y. and Smith,S.S. (2005) Transgene-induced CCWGG methylation does not alter CG methylation patterning in human kidney cells. *Nucleic Acids Res.*, **33**, 6124–6136.
31. Chaplin,M.F. and Bucke,C. (1990) *Enzyme Technology*. Cambridge University Press, Cambridge, UK.
32. Friedman,S. (1979) The effect of 5-azacytidine on E. coli DNA methylase. *Biochem. Biophys. Res. Commun.*, **89**, 1328–1333.

33. Lin,K.T., Momparler,R.L. and Rivard,G.E. (1981) High-performance liquid chromatographic analysis of chemical stability of 5-aza-2′-deoxycytidine. *J. Pharm. Sci.*, **70**, 1228–1232.

34. Chan,K.K., Giannini,D.D., Staroscik,J.A. and Sadee,W. (1979) 5-Azacytidine hydrolysis kinetics measured by high-pressure liquid chromatography and 13C-NMR spectroscopy. *J. Pharm. Sci.*, **68**, 807–812.

35. Clark,J., Shevchuk,T., Kho,M.R. and Smith,S.S. (2003) Methods for the design and analysis of oligodeoxynucleotide-based DNA (cytosine-5) methyltransferase inhibitors. *Anal. Biochem.*, **321**, 50–64.

36. Cheng,J.C., Yoo,C.B., Weisenberger,D.J., Chuang,J., Wozniak,C., Liang,G., Marquez,V.E., Greer,S., Orntoft,T.F., Thykjaer,T. *et al.* (2004) Preferential response of cancer cells to zebularine. *Cancer Cell*, **6**, 151–158.

37. Zhou,L., Cheng,X., Connolly,B.A., Dickman,M.J., Hurd,P.J. and Hornby,D.P. (2002) Zebularine: a novel DNA methylation inhibitor that forms a covalent complex with DNA methyltransferases. *J. Mol. Biol.*, **321**, 591–599.

38. Goodman,M.F. (1997) Hydrogen bonding revisited: geometric selection as a principal determinant of DNA replication fidelity. *Proc. Natl Acad. Sci. USA*, **94**, 10493–10495.

39. Ehrlich,M., Jackson,K. and Weemaes,C. (2006) Immunodeficiency, centromeric region instability, facial anomalies syndrome (ICF). *Orphanet. J. Rare Dis.*, **1**, 2.

40. Paz,M.F., Fraga,M.F., Avila,S., Guo,M., Pollan,M., Herman,J.G. and Esteller,M. (2003) A systematic profile of DNA methylation in human cancer cell lines. *Cancer Res.*, **63**, 1114–1121.

41. Ibragimova,I., Ibanez de Caceres,I., Hoffman,A.M., Potapova,A., Dulaimi,E., Al-Saleem,T., Hudes,G.R., Ochs,M.F. and Cairns,P. (2010) Global reactivation of epigenetically silenced genes in prostate cancer. *Cancer Prev. Res.*, **3**, 1084–1092.

42. Beisler,J.A., Abbasi,M.M., Kelley,J.A. and Driscoll,J.S. (1977) Synthesis and antitumor activity of dihydro-5-azacytidine, a hydrolytically stable analogue of 5-azacytidine. *J. Med. Chem.*, **20**, 806–812.

43. Bouzon,M. and Marliere,P. (1997) Human deoxycytidine kinase as a conditional mutator in Escherichia coli. *C R Acad. Sci. III*, **320**, 427–434.

44. Momparler,R.L., Bouffard,D.Y., Momparler,L.F., Dionne,J., Belanger,K. and Ayoub,J. (1997) Pilot phase I-II study on 5-aza-2′-deoxycytidine (Decitabine) in patients with metastatic lung cancer. *Anticancer Drugs*, **8**, 358–368.

45. Juergens,R.A., Wrangle,J., Vendetti,F.P., Murphy,S.C., Zhao,M., Coleman,B., Sebree,R., Rodgers,K., Hooker,C.M., Franco,N. *et al.* (2011) Combination epigenetic therapy has efficacy in patients with refractory advanced non-small cell lung cancer. *Cancer Discov.*, **1**, 598–607.

46. Smith,S.S. and Crocitto,L. (1999) DNA methylation in eukaryotic chromosome stability revisited: DNA methyltransferase in the management of DNA conformation space. *Mol. Carcinog.*, **26**, 1–9.

47. Smith,S.S. (2000) Gilbert′s conjecture: the search for DNA (cytosine-5) demethylases and the emergence of new functions for eukaryotic DNA (cytosine-5) methyltransferases. *J. Mol. Biol.*, **302**, 1–7.

48. Kantarjian,H., Issa,J.P., Rosenfeld,C.S., Bennett,J.M., Albitar,M., DiPersio,J., Klimek,V., Slack,J., de Castro,C., Ravandi,F. *et al.* (2006) Decitabine improves patient outcomes in myelodysplastic syndromes: results of a phase III randomized study. *Cancer*, **106**, 1794–1803.

49. Alva,A.S., Hahn,N.M., Aparicio,A.M., Singal,R., Yellapragada,S. and Sonpavde,G. (2011) Hypomethylating agents for urologic cancers. *Future Oncol.*, **7**, 447–463.

50. Hatoum,H.T., Lin,S.J., Buchner,D. and Kim,E. (2011) Use of hypomethylating agents and associated care in patients with myelodysplastic syndromes: a claims database study. *Curr. Med. Res. Opin.*, **27**, 1255–1262.